

Influence of Cations on the Vibrational Spectra and Structure of [WO₄] Complexes in Molten Tungstates

Yu. K. Voron'ko and A. A. Sobol'

Laser Materials and Technologies Research Center, Prokhorov General Physics Institute, Russian Academy of Sciences, ul. Vavilova 38, Moscow, 119991 Russia

e-mail: sobol@lst.gpi.ru

Received January 26, 2004; in final form, November 23, 2004

Abstract—The vibrational spectra and structure of isolated [WO₄]²⁻ anions in molten alkali, alkaline-earth, rare-earth, Pb, Bi, Zn, Sc, and Cd tungstates are studied by high-temperature Raman spectroscopy. The degenerate modes of the [WO₄]²⁻ anion in K–Gd tungstate melts are found to be split, which is interpreted in terms of the symmetry of the cation environment of the [WO₄]²⁻ anion in the melts. The frequency of the fully symmetric stretching mode (ν_1) of the [WO₄]²⁻ group in molten tungstates is examined in relation to the polarizing power P and electronegativity γ of the cation. The origin of the nonmonotonic variation of ν_1 with P and γ for the tungstate melts studied is discussed.

INTRODUCTION

Raman spectroscopy of covalently bonded anion groups, such as [NO₃], [CO₃], and [SO₄], was widely used earlier to study the influence of cations (M^{z+}) on the vibrational spectra and structure of metal–oxygen complexes in melts [1–5]. The nature of the cation was found to have a significant effect on the stretching frequencies of [RO_m]^{p-} groups, which are known to persist in melts.

In the 1960s–1970s, many studies were concerned with the effect of the M^{z+} cation on the frequency of the symmetric stretching mode ν_1 in [RO_m]^{p-} complexes in melts [1–5]. It was concluded in those studies that partially covalent M^{z+}–O bonds involving oxygens of [RO_m]^{p-} influence the force constants of the R–O bond. In light of this, considerable effort was focused on the dependence of ν_1 on the degree of covalent bonding between M^{z+} and oxygen, which was quantified using different functions. In particular, Janz *et al.* [5] used the ionic potential $A = z/r$, where z is the charge of the M^{z+} cation and r is its ionic radius. It was also proposed [1–4] that the potential A should be corrected using the shielding constant S_{eff} of the M^{z+} cation,

$$S_{\text{eff}} = (5z^{1.27})/(r^{1/2}I),$$

where I is the ionization potential.

Several approaches to correcting A were discussed in the literature. For example, Janz *et al.* [1, 5] used polarizing power, $P = AS_{\text{eff}}$, as y . By contrast, Brooker and Breiding [3] defined P as A/S_{eff} and used the func-

tion $y = \log(P\alpha)$, where α is the polarizability of the M^{z+} cation.

Note that, in those studies, efforts were aimed at finding such a characteristic y that ν_1 would be a linear function of y , without paying attention to the physical meaning of y [1–5]. Although the expressions for P and A incorporated the values of r , I , and α determined for M^{z+} cations in crystals, rather in melts, the dependences of ν_1 on y obtained in [1–5] were monotonic, or even linear, for some melts. Those results, however, provided no fundamental understanding of the influence of M^{z+} cations on the vibrational spectra of [RO_m]^{p-} complexes in melts because experimental data were only obtained for a narrow range of systems, with Group I M^{z+} cations.

Systematic studies of melts containing M^{z+} ions in other oxidation states were difficult to carry out in the 1960s–1970s because, at that time, Raman measurements at temperatures above 1200 K required very much effort.

Our group has developed a technique and experimental setup for Raman scattering studies of melts at temperatures of up to 2000 K [6], which has made it possible to measure the Raman spectra of a far broader range of melts. The objective of this work was to investigate the effects of various M^{z+} cations on the vibrational spectra and structure of anion complexes in melts. As [RO_m]^{p-} complexes, we chose [WO₄]²⁻ tetrahedral groups because tungstate melts exist for a wide variety of metals. As reported earlier [7], the nature of the M^{z+} cation influences the stretching frequencies of [RO_m]^{p-} complexes not only in melts but also in crystals

Frequency ν of the fully symmetric mode of the $[\text{WO}_4]^{2-}$ anion in $\text{M}_2^z\text{O}_z \cdot z\text{WO}_3$ melts

Metal	Atomic weight	Electronegativity [18]	ν , cm^{-1}	
			1670 K	1920 K
Li	6.94	0.67	922	
Na	22.9	0.56	914	
K	39.1	0.446	906	
Cs	132.9	0.22	888	
Mg	24.3	1.318	962	956
Ca	40.1	0.946	929***	923
Sr	87.6	0.721	922***	916
Ba	137.33	0.651	912***	906
Sc	44.9	1.75*	959***	953
Gd	157.2	1.75*	952	947
Yb	173.0	1.55*	962**	956
Zn	65.38	2.22	962	
Cd	112.41	1.98	936	
Pb	207.2	2.29	916	
Bi	209	2.34	925	

* Pauling electronegativity values [19] converted to the Sanderson scale [18].

** Supercooled melt.

*** Frequencies obtained by extrapolation at a melt temperature of 1670 K.

and glasses. Tungstate crystals are effective gain media for Raman lasers [8–11], in which the vibrational frequencies of $[\text{WO}_4]^{2-}$ complexes are used for frequency conversion. Therefore, the study of the effect of M^{z+} cations on the frequencies of $[\text{WO}_4]^{2-}$ complexes in melts is also of interest for designing crystalline media for tungstate Raman lasers.

In addition, the study of tungstate melts makes it possible to examine the possibility of the formation of clusters made up of $[\text{RO}_m]^{p-}$ complexes and M^{z+} cations. Some cation environments may distort the symmetry of the $[\text{RO}_m]^{p-}$ anion from the “free-anion” symmetry. Such distortions must split the degenerate vibrational modes of $[\text{RO}_m]^{p-}$, which can be observed readily in the Raman spectrum. In the case of weak cation–anion interaction and random arrangement of cations around $[\text{RO}_m]^{p-}$ groups, the effect will be insignificant. The splitting of vibrational modes degenerate in the “free $[\text{NO}_3]$ anion” approximation was only observed in the Raman spectra of molten Li and Ag nitrates [1]. In the Raman spectra of other alkali nitrates, as well as in the spectra of alkali sulfates and carbonates, such effects were indiscernible. Therefore, our Raman scattering studies of a wide range of molten tungstates, with

various cations, provide additional insight into the cation environment of $[\text{RO}_m]^{p-}$ anions in melts.

EXPERIMENTAL AND RESULTS

Samples and characterization techniques. Samples for this investigation were prepared by melting appropriate mixtures of WO_3 and M_2O_z (M = Group I–V elements) in platinum crucibles. The W : O atomic ratio in the tungstates studied (table) is 1 : 4, which implies the possibility of the formation of isolated $[\text{WO}_4]^{2-}$ groups.

Room-temperature Raman spectra were measured by a standard procedure on a Spex Ramalog 1403 spectrophotometer, using the 488-nm Ar laser line for excitation. High-temperature Raman scattering studies of tungstate melts were carried out at temperatures of up to 2000 K in air [6]. The samples were placed in 5-mm-diameter platinum crucibles and melted in vertical tubular Pt–30% Rh wound furnaces. Excitation was provided by a copper vapor laser (510.4 nm, pulse repetition rate of 15 kHz). Polarized Raman spectra were recorded in a backscattering geometry: both the exciting beam and scattered radiation passed through the melt surface.

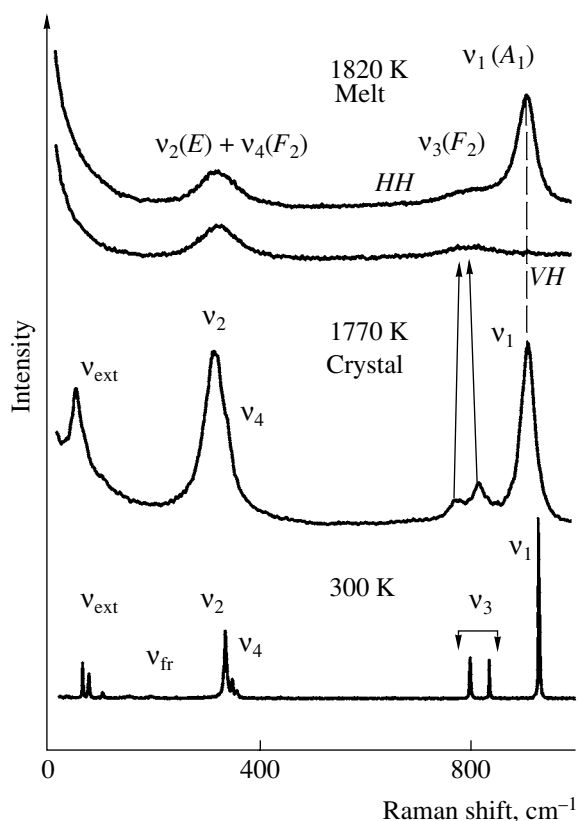


Fig. 1. Effect of heating and melting on the Raman spectrum of BaWO_4 in HH (parallel polarizers) and VH (crossed polarizers) scattering geometries; ν_1 – ν_4 are the internal modes of a “free” $[\text{WO}_4]^{2-}$ tetrahedral anion, ν_{fr} is a rotational mode, and ν_{ext} is an external mode.

Raman spectra of crystalline and molten tungstates containing different M^{2+} cations. The scheelite structure is a convenient model system for studying the vibrational spectrum of isolated $[\text{WO}_4]^{2-}$ tetrahedral complexes [12]. The $[\text{WO}_4]^{2-}$ group in the scheelite structure possesses tetragonal site symmetry, which leads to splitting of the vibrational modes of this complex compared to a “free” $[\text{WO}_4]^{2-}$ anion (cubic symmetry). The splitting of the degenerate modes $\nu_2(E)$, $\nu_3(F_2)$, and $\nu_4(F_2)$ is well observed in the Raman spectra of crystalline scheelites. In particular, the $\nu_3(F_2)$ mode splits into two components, E_g and B_g , with $\Delta\nu = 30$ – 40 cm^{-1} [11, 12]. The tetragonal crystal field in crystalline scheelites does not split the fully symmetric nondegenerate mode $\nu_1(A_1)$, but its frequency may depend on the separation between $[\text{WO}_4]^{2-}$ complexes in the crystal owing to the Davydov splitting [11]. Since the crystal field and Davydov splitting effects are missing in melts, their Raman spectra must show a set of modes of a free $[\text{WO}_4]^{2-}$ anion, as observed in the spectra of molten alkaline-earth tungstates [11, 13].

This is illustrated in Fig. 1 by the example of barium tungstate. The Raman spectrum of its melt shows only

the internal modes $\nu_1(A_1)$, $\nu_2(E)$, $\nu_3(F_2)$, and $\nu_4(F_2)$ of the $[\text{WO}_4]^{2-}$ group, which are all unsplit, in contrast to those in crystals. Melting does not change the $\nu_1(A_1)$ frequency to within 1 cm^{-1} , which attests to a small Davydov splitting of this mode in the structure of BaWO_4 [11]. The $\nu_1(A_1)$ band in the Raman spectrum of molten barium tungstate is fully polarized in both the VH (crossed polarizers) and HH (parallel polarizers) geometries. This effect is only possible for a tetrahedral complex possessing cubic symmetry. The Raman spectrum of BaWO_4 , illustrating internal modes in a tetrahedral $[\text{WO}_4]^{2-}$ complex of cubic symmetry (Fig. 1), can be used to identify similar complexes in other tungstate melts, if their spectrum will be similar to that of BaWO_4 .

This fact is useful in studying the structure of W-O complexes in the melt of those tungstates that contain no isolated $[\text{WO}_4]^{2-}$ groups in the crystalline state, in contrast to crystalline scheelites. Among such tungstates are ZnWO_4 and MgWO_4 (wolframite structure), in which the main building block is a $[\text{W}_2\text{O}_8]$ ribbon made up of tetrahedra [14, 15]. Raman scattering by the internal modes of the wolframite ribbon have been studied in less detail compared to $[\text{WO}_4]^{2-}$ tetrahedral groups. The 300-K spectra of ZnWO_4 and MgWO_4 show a set of peaks due to the large number of vibrational degrees of freedom in the ribbon anion (Fig. 2). The strongest, high-frequency peak in these spectra is assignable to stretches of the W-O end group.

As seen in Fig. 2a, melting produces marked changes in the Raman spectrum of ZnWO_4 , which becomes very similar to the spectra of melts containing isolated $[\text{WO}_4]^{2-}$ groups. The transformation of the $[\text{W}_2\text{O}_8]$ ribbon into isolated $[\text{WO}_4]^{2-}$ tetrahedra upon ZnWO_4 melting is evidenced by the considerable difference in frequency ($\Delta \approx 60 \text{ cm}^{-1}$) between the strongest, high-frequency peak in the spectrum of crystalline ZnWO_4 before melting and the $\nu_1(A_1)$ mode of the $[\text{WO}_4]^{2-}$ anion in the melt (Fig. 2a). The Raman spectrum of MgWO_4 , another tungstate with the wolframite structure, provides conclusive evidence that, above the melting point, the W-O complexes in the melt have the form of isolated $[\text{WO}_4]^{2-}$ groups. In contrast to ZnWO_4 , the transformation of the $[\text{W}_2\text{O}_8]$ ribbons into $[\text{WO}_4]^{2-}$ complexes in MgWO_4 occurs in the crystalline state, as a result of the $\beta \rightarrow \alpha$ phase transition, as demonstrated by the changes in the Raman spectrum of MgWO_4 during heating (Fig. 2b). The $\beta \rightarrow \alpha$ phase transition of MgWO_4 is accompanied by a marked shift ($\Delta \approx 60 \text{ cm}^{-1}$) of the strongest, high-frequency peak, similar to what occurs in the Raman spectrum of ZnWO_4 on melting. Melting has little effect on the $\nu_1(A_1)$ frequency in the Raman spectrum of α - MgWO_4 because the $[\text{WO}_4]^{2-}$ anion retains its tetrahedral structure.

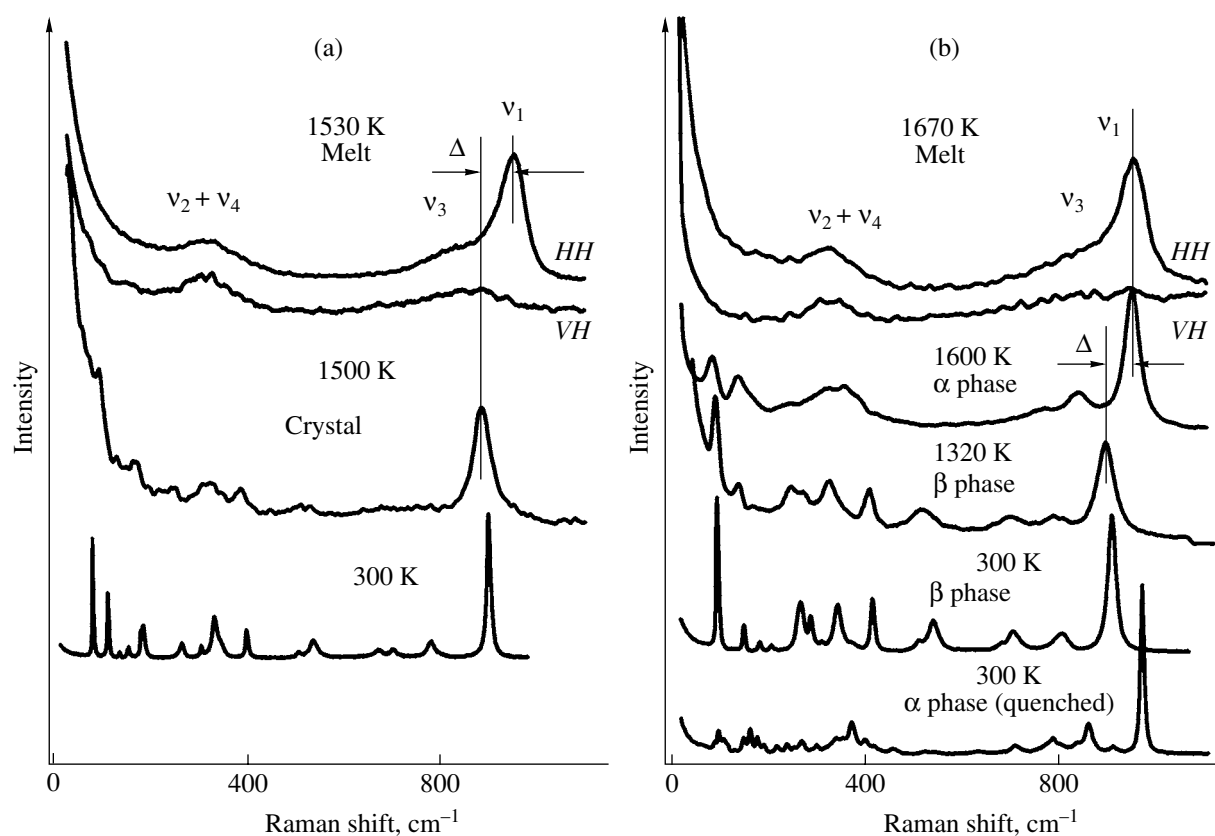


Fig. 2. Effect of heating and melting on the Raman spectra of (a) ZnWO_4 and (b) MgWO_4 in HH (parallel polarizers) and VH (crossed polarizers) scattering geometries; ν_1 – ν_4 are the internal modes of a “free” $[\text{WO}_4]^{2-}$ tetrahedral anion.

The high-temperature phase α - MgWO_4 can be frozen-in at 300 K by rapid quenching from the liquid state (Fig. 2b). The pronounced dissimilarity between the 300-K Raman spectra of α - and β - MgWO_4 , in particular the large difference in frequency ($\Delta \approx 60 \text{ cm}^{-1}$) between the $\nu_1(A_1)$ mode of the $[\text{WO}_4]^{2-}$ tetrahedral group and the high-frequency Raman band arising from the $[\text{W}_2\text{O}_8]$ wolframite ribbon clearly demonstrates that the chemical environment of W must be taken into account in analyzing the effect of the cation on the vibrational spectra of W–O groups. Such analysis requires Raman data for several tungstates containing W–O complexes identical in structure (e.g., tetrahedral). Note in this context that the conclusions made by Gallucci *et al.* [16] appear unjustified because they examined the effect of the M^{z+} cation on the frequencies of internal modes in W–O complexes in crystalline tungstates without taking into account the structure of the complexes.

The number of crystalline tungstates containing W–O groups identical in structure is not very large, which limits the range of systems for studying the effect of cations on the vibrational spectra of anion complexes. Our Raman scattering studies indicate that $\text{M}_2^{z+}\text{O}_z \cdot z\text{WO}_3$ melts with $z = 1$ – 3 contain identical anions—iso-

lated $[\text{WO}_4]^{2-}$ tetrahedra— independent of whether or not $\text{M}_2\text{O}_z \cdot z\text{WO}_3$ crystals contain isolated $[\text{WO}_4]^{2-}$ groups. Thus, $\text{M}_2\text{O}_z \cdot z\text{WO}_3$ tungstate melts are the only model systems suitable for analyzing the effect of various M^{z+} cations on the spectrum of internal vibrations of isolated tetrahedral $[\text{WO}_4]^{2-}$ groups.

Figure 3 shows the Raman spectra of several $\text{M}_2\text{O}_z \cdot z\text{WO}_3$ melts. The spectra each contain four features, arising from internal modes of isolated $[\text{WO}_4]^{2-}$ anions. The feature due to the fully symmetric mode $\nu_1(A_1)$ is fully polarized. The M^{z+} cation has no effect on the shape of the Raman spectra from $\text{M}_2\text{O}_z \cdot z\text{WO}_3$ melts but influences the frequency of the fully symmetric mode $\nu_1(A_1)$.

We examined the dependence of this frequency on the polarizing power P for several M^{z+} cations (Fig. 4a) in comparison with analogous data for molten alkali nitrates [1–3, 5]. Since Lazarev *et al.* [7] assumed that changes in the frequency of the fully symmetric mode ν_1 of $[\text{RO}_m]^{p-}$ groups are caused by the effect of partially covalent M^{z+} –O bonds involving oxygens of $[\text{RO}_m]^{p-}$ groups, it is of interest to analyze the dependence of $\nu_1(A_1)$ on the electronegativity γ of M^{z+} cations. Such dependences were not examined in studies of nitrates,

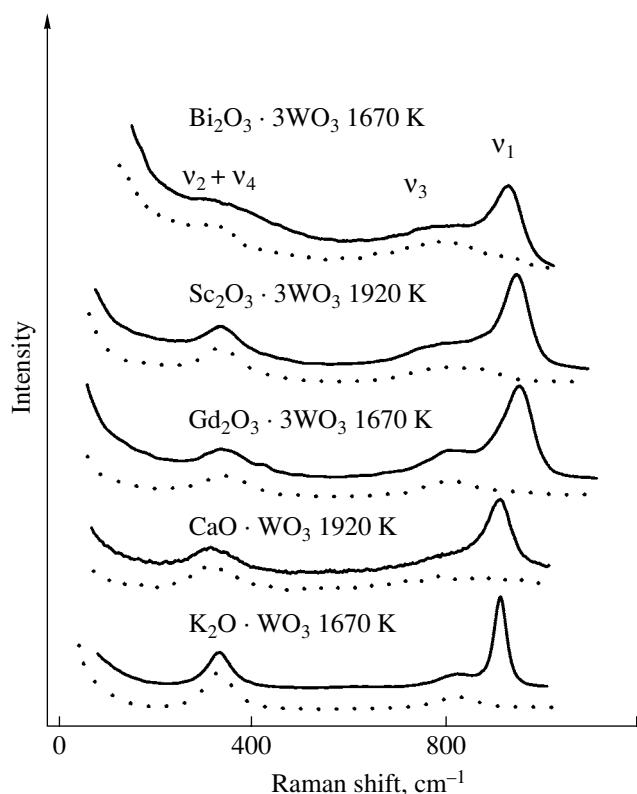


Fig. 3. Raman spectra of melts containing $[\text{WO}_4]^{2-}$ tetrahedral anions and different M^{z+} cations; HH (solid lines) and VH (dotted lines) scattering geometries; v_1 – v_4 are the internal modes of a “free” $[\text{WO}_4]^{2-}$ tetrahedral anion.

sulfates, or carbonates [1–5] but were widely used in interpreting the variations in the frequencies of internal modes of organic complexes [17].

Figure 4b shows the plot of $\nu_1(A_1)$ versus electronegativity γ of M^{z+} cations for the tungstate melts studied. For most M^{z+} cations, γ values were taken from [18] (Sanderson scale). The electronegativity values for Gd, Yb, and Sc were taken from [19] (Pauling scale) and converted to the Sanderson scale using an equation from [20]. Since Raman frequencies are temperature-dependent by virtue of anharmonicity effects, the $\nu_1(A_1)$ frequencies in Figs. 4a and 4b are reduced to the same temperature, 1670 K.

The Raman spectra for melts of (refractory) Ca, Sr, Ba, Sc, and Yb tungstates were measured at 1920 K. In Figs. 4a and 4b, the $\nu_1(A_1)$ frequency for these melts was extrapolated to 1670 K under the assumption that $\nu_1(A_1)$ is a linear function of temperature. The table lists the measured 1920-K $\nu_1(A_1)$ frequencies and the values found by extrapolation to 1670 K. Since the $\text{Yb}_2\text{O}_3 \cdot 3\text{WO}_3$ melt had a pronounced tendency to supercool, it was possible to experimentally determine $\nu_1(A_1)$ at both 1920 and 1670 K.

The Raman spectra for all of the tungstate melts studied correspond to a cubic free $[\text{WO}_4]^{2-}$ anion, as evidenced by the unsplit degenerate internal modes $\nu_2(E)$, $\nu_3(F_2)$, and $\nu_4(F_2)$ and the high degree of polarization of the $\nu_1(A_1)$ mode of the $[\text{WO}_4]^{2-}$ anion (Fig. 3), independent of the oxidation state and electronegativity of the M^{z+} cation ($z = 1$ – 3). One possible reason is that no complexation occurs in the melts because of the weak cation–anion interaction. On the other hand, the $[\text{WO}_4]^{2-}$ groups in the melt may also retain cubic symmetry in the case of complexation if the cation environment of the $[\text{WO}_4]^{2-}$ anions, due to partially covalent M–O bonds, possesses cubic or higher symmetry. This appears likely for tungstates containing one type of M^{z+} cation. At the same time, if the nearest neighbor environment of the $[\text{WO}_4]^{2-}$ groups is formed by dissimilar M^{z+} cations, the symmetry of $[\text{WO}_4]^{2-}$ may be lower than cubic because of the asymmetric distortion of its structure. This prompted us to measure the Raman spectra of $x\text{K}_2\text{O} \cdot (1-x)\text{Gd}_2\text{O}_3 \cdot (3-2x)\text{WO}_3$ tungstate melts with $x = 0$ – 1 . In such melts, the cation environment of the $[\text{WO}_4]^{2-}$ anion may have several configurations, differing in cation composition (x), in particular those with $x = 0$ or 1.

The Raman spectra of the melts with x from 0 ($\text{Gd}_2\text{O}_3 \cdot 3\text{WO}_3$) to 1 ($\text{K}_2\text{O} \cdot \text{WO}_3$) are displayed in Fig. 5 for two scattering geometries (parallel and crossed polarizers). Since the $\nu_1(A_1)$ mode of the $[\text{WO}_4]^{2-}$ tetrahedron is singly degenerate, it does not split upon distortions of the cubic symmetry around the free anion. Therefore, the $\nu_1(A_1)$ band cannot be used to reveal cation–anion complexation in mixed-cation tungstate melts. With increasing x in $x\text{K}_2\text{O} \cdot (1-x)\text{Gd}_2\text{O}_3 \cdot (3-2x)\text{WO}_3$, the $\nu_1(A_1)$ frequency varies monotonically (Fig. 5a). As shown earlier [21], $\nu_1(A_1)$ is a nonlinear function of x ($\text{K}^+ : \text{Gd}^{3+}$ ratio in the melt) because the $[\text{WO}_4]^{2-}$ group is more likely to be coordinated to Gd^{3+} than to K^+ .

In contrast, the triply degenerate mode $\nu_3(F_2)$ may split in response to a reduction in the symmetry of the $[\text{WO}_4]^{2-}$ anion. This does occur in the Raman spectra of mixed-cation tungstate melts (Fig. 5b). Unsplit $\nu_3(F_2)$ modes, at nearly the same frequency, were only observed in the spectra of the $\text{K}_2\text{O} \cdot \text{WO}_3$ ($x = 1$) and $\text{Gd}_2\text{O}_3 \cdot 3\text{WO}_3$ ($x = 0$) melts (Fig. 5b), indicating that the $[\text{WO}_4]^{2-}$ anion retains cubic symmetry in melts containing one type of cation. In the spectra of the mixed-cation ($\text{Gd}^{3+} + \text{K}^+$) tungstate melts with $x = 0.67$ – 0.85 , the $\nu_3(F_2)$ band comprises several components (Fig. 5b). Subtracting the $\nu_3(F_2)$ band in the spectrum of the $x = 0$ melt from that for $x < 0.7$, we obtain a well-defined $\nu_3(F_2)$ doublet, labeled L in Fig. 5b. The doublet can also be obtained by subtracting the $\nu_3(F_2)$ band in the spectrum of the $x = 1$ melt from the composite $\nu_3(F_2)$ band in the spectra for $x > 0.7$ (Fig. 5b). The dou-

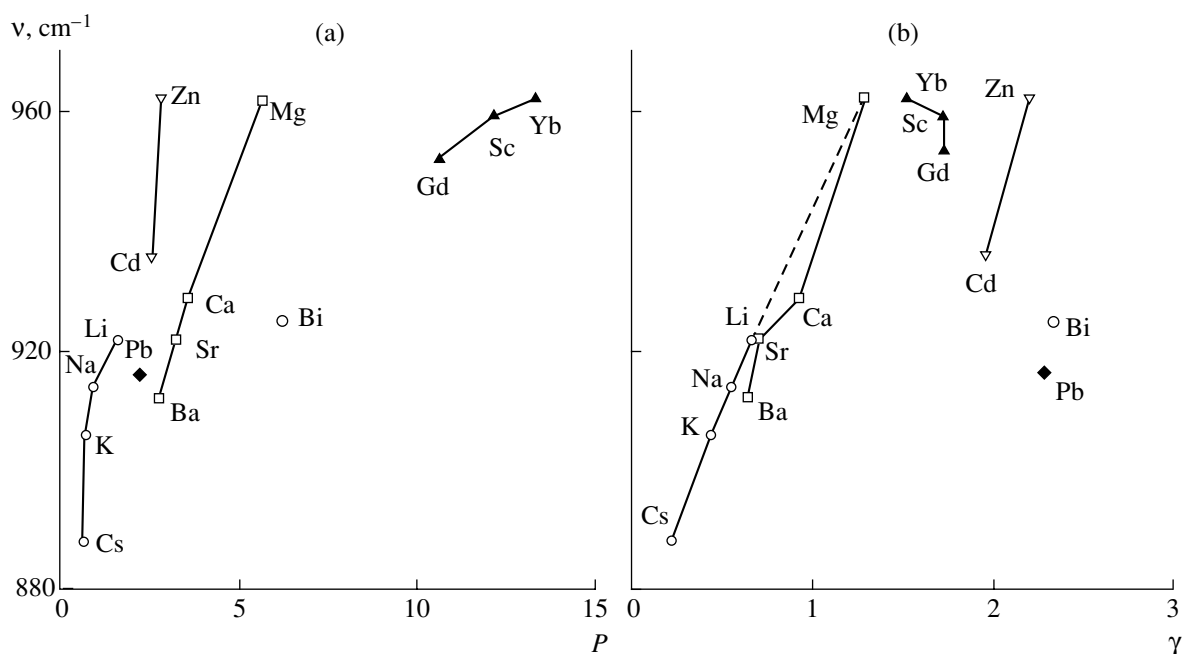


Fig. 4. Frequency of the fully symmetric mode $\nu_1(A_1)$ of the $[\text{WO}_4]^{2-}$ anion as a function of the (a) polarizing power $P = AS_{\text{eff}}$ and (b) electronegativity γ of the M^{z+} cation for $M_2O_z \cdot z\text{WO}_3$ melts.

plet splitting of the $\nu_3(F_2)$ band is the signature for distortion of the cubic symmetry around the $[\text{WO}_4]^{2-}$ anion.

A similar splitting of the $\nu_3(F_2)$ mode is well-defined in the Raman spectra of crystalline scheelites, in which the incorporation of the $[\text{WO}_4]^{2-}$ anion into the crystal lattice reduces the symmetry of the anion to tetragonal one (Fig. 1). Thus, the spectra in Fig. 5b indicate that $x\text{K}_2\text{O} \cdot (1-x)\text{Gd}_2\text{O}_3 \cdot (3-2x)\text{WO}_3$ melts contain $[\text{WO}_4]^{2-}$ groups in different cation environments. In contrast to that in $\text{K}_2\text{O} \cdot \text{WO}_3$ and $\text{Gd}_2\text{O}_3 \cdot 3\text{WO}_3$ melts, the cation environment of the $[\text{WO}_4]^{2-}$ complexes in mixed tungstate melts has lower-than-cubic symmetry. The relative concentration of low-symmetry L groups depends on x ($\text{K}^+ : \text{Gd}^{3+}$ ratio in the melt): it reaches a maximum in the range $x = 0.67-0.75$ and drops to zero at $x = 0$ and 1 (Fig. 5b).

DISCUSSION

The present results attest to significant cation–anion interaction in tungstate melts containing isolated $[\text{WO}_4]^{2-}$ groups, which determines the symmetry of their cation environment. At the same time, this effect cannot be interpreted as evidence for the existence of crystal-like fragments made up of M^{z+} cations and $[\text{WO}_4]^{2-}$ anions because the Raman spectra show only modes of the $[\text{WO}_4]^{2-}$ anion slightly distorted by the M^{z+} cation, while the $M^{z+}-[\text{WO}_4]^{2-}$ and $M^{z+}-\text{O}^{2-}$ stretching modes are missing. These features of the

spectra suggest that the energy of the cation–anion bonds is low compared to that of the strong covalent bonds within the $[\text{WO}_4]^{2-}$ complex. Therefore, the effect of cations on the spectrum of internal vibrations of $[\text{WO}_4]^{2-}$ anions can be interpreted in terms of the competition between the association and dissociation of M^{z+} cations and $[\text{WO}_4]^{2-}$ anions, the process being dominated by dissociation. The partially covalent bonding between M^{z+} and oxygens of $[\text{WO}_4]^{2-}$ anions implies that the structure, interatomic distances, and bond angles remain unchanged after the bonds broken in the process of association–dissociation are restored. This accounts for the observed effect of cation environment on the structure of free $[\text{WO}_4]^{2-}$ groups. In the instance of purely ionic bonding, a randomly restructuring cation environment would produce an average, spherically symmetric electric field, incapable of distorting the cubic symmetry of the free $[\text{WO}_4]^{2-}$ complex.

Consider the effect of the M^z cation on the $\nu_1(A_1)$ frequency of the $[\text{WO}_4]^{2-}$ complex in $M_2O_z \cdot z\text{WO}_3$ melts. As seen in Fig. 4a, the dependences of $\nu_1(A_1)$ on the polarizing power of the M^{z+} cation are represented by several plots, demonstrating a monotonic variation of $\nu_1(A_1)$ with P only within a given group of the Periodic Table. Therefore, there is no point in seeking a universal expression for P which might reveal a general correlation between $\nu_1(A_1)$ and P for a wide variety of M^{z+} cations. This may be associated to some extent with a number of controversial points in the use of parameters appearing in P , as discussed above. The dependences of

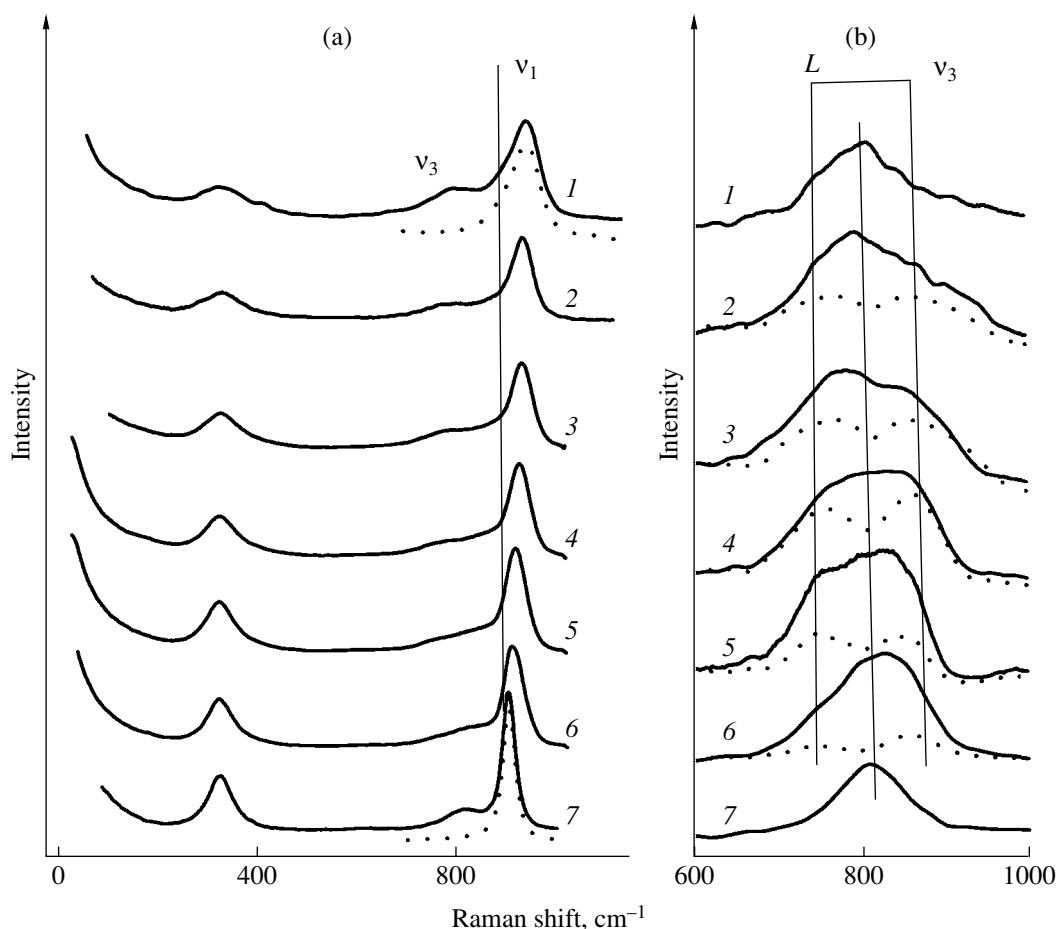


Fig. 5. Raman spectra of $x\text{K}_2\text{O} \cdot (1-x)\text{Gd}_2\text{O}_3 \cdot (3-2x)\text{WO}_3$ melts with $x = (1)$ 0, (2) 0.5, (3) 0.67, (4) 0.75, (5) 0.85, (6) 0.92, and (7) 1; (a) HH scattering geometry (the dotted lines show the ν_1 band obtained for the $\text{K}_2\text{O} \cdot \text{WO}_3$ ($x = 1$) and $\text{Gd}_2\text{O}_3 \cdot 3\text{WO}_3$ ($x = 0$) melts by subtracting the spectrum obtained in the VH scattering geometry from the spectrum in the HH geometry); (b) VH geometry (L is the $\nu_3(F_2)$ mode, which undergoes doublet splitting in mixed-cation melts).

$\nu_1(A_1)$ on the electronegativity γ of M^{z+} cations are more regular (Fig. 4b). In particular, $\nu_1(A_1)$ is an almost linear function of γ for the Group I and II M^{z+} cations. At the same time, the $\nu_1(A_1)$ versus γ data for other groups of the Periodic Table do not fit in with this tendency. The values of $\nu_1(A_1)$ for Group III and IV elements are substantially lower than would be expected, especially for the heavy cations Bi^{3+} and Pb^{2+} . One possible explanation is that γ is difficult to accurately determine for elements with complex electron shells. There are also a number of other possible reasons for the observed variation of $\nu_1(A_1)$ with γ .

Consider the mechanism underlying the distortion of the fully symmetric $\nu_1(A_1)$ mode of the $[\text{WO}_4]^{2-}$ anion in certain cation environments. The energy of this mode in the free $[\text{WO}_4]^{2-}$ complex approximation can be written in the form

$$E \approx \frac{1}{2\pi} \sqrt{\frac{k_1}{m}}, \quad (1)$$

where k_1 is the force constant of the W–O bond and m is the reduced mass (equal to the atomic mass of oxygen in the case under consideration). The atomic mass of W is here left out of account because, in tetrahedral complexes of cubic and tetragonal symmetries, the W atoms are not involved in the $\nu_1(A_1)$ vibrations. In a number of studies [3, 9], partially covalent bonding of cations was assumed to have a significant effect on the force constants of the anion complex only. Since the M^{z+} cation is bonded, albeit only dynamically, to an oxygen of a $[\text{WO}_4]^{2-}$ complex, m must be corrected for M^{z+} –O bonding. The energy of the $\nu_1(A_1)$ mode then has the form

$$E \approx \frac{1}{2\pi} \sqrt{\frac{k^*}{m^*}}. \quad (2)$$

Here, $k^* = k_1 + \Delta k_M(\gamma)$, where k_1 is the force constant in (1) and $\Delta k_M(\gamma)$ is the change in the force constant of the W–O bond due to the inductive effect of the par-

tially covalent bond with the M^{z+} cation. The $\Delta k_M(\gamma)$ value depends on the electronegativity γ of the M^{z+} cation. The atomic mass m^* in (2) can be written as $m^* = m_O + \Delta m_M(\gamma)$, where $\Delta m_M(\gamma)$ takes into account the correction for the dynamic M^{z+} -O bonding. The value of $\Delta m_M(\gamma)$ depends on both the atomic mass of the M^{z+} cation and the M^{z+} -O bond energy, which can be estimated from the electronegativity of M^{z+} . Thus, partially covalent bonding of the M^{z+} cation will influence both the numerator and the denominator in Eq. (2). Therefore, an increase in the electronegativity of M^{z+} may be accompanied by a rise in ν_1 because of the increase in numerator in (2). At the same time, this increase may be slowed down because of the changes in m^* in the denominator in (2).

These observations shed some light on the origin of the observed variation of $\nu_1(A_1)$ with γ (Fig. 4b). For molten tungstates of alkali and alkaline-earth metals with low γ values, the correction to m^* is insignificant, and the linear rise in $\nu_1(A_1)$ with γ is mainly due to the effect of the partially covalent bonding of the M^{z+} cation on the force constants of the fully symmetric mode. In going from Cs^+ to Mg^{2+} , $\nu_1(A_1)$ increases from 888 to 962 cm^{-1} . Further rise in $\nu_1(A_1)$ with γ (rare-earth and zinc tungstates) is impossible because of the correction of m^* in the denominator in Eq. (2). Finally, for heavy M^{z+} cations with relatively high values of γ (Cd, Pb, and Bi), $\nu_1(A_1)$ decreases with increasing γ because of the increase in m^* (Fig. 4b). The M^{z+} cation may have a similar effect on the $\nu_1(A_1)$ frequency of the $[WO_4]^{2-}$ complex in crystalline tungstates containing isolated $[WO_4]^{2-}$ groups, in which the crystal-field and Davydov splitting effects are weak. For example, we observed a monotonic increase in $\nu_1(A_1)$ (in the range 916–941 cm^{-1}) for crystalline tungstates (Cs–Li), just as in the melts. Among the tungstates studied, the highest $\nu_1(A_1)$ frequency (975 cm^{-1}) was observed in molten and crystalline (α form) $MgWO_4$ (Fig. 2). The spectrum of crystalline $PbWO_4$ showed a low $\nu_1(A_1)$ frequency, 905 cm^{-1} , characteristic of melts containing heavy cations with relatively high electronegativity values.

Note that the effect of the electronegativity of M^{z+} cations on the $\nu_1(A_1)$ frequency may be obscured severely by Davydov splitting, which takes place in a number of crystalline tungstates. In particular, in the case of $BaWO_4$, $SrWO_4$, and $CaWO_4$, $\nu_1(A_1)$ was observed to increase in going from Ba to Ca (with increasing γ) for melts and to decrease for crystalline materials [11].

CONCLUSIONS

The nature of the M^{z+} cation has a significant effect on the frequency of the fully symmetric mode $\nu_1(A_1)$ of isolated $[WO_4]^{2-}$ anions in tungstate melts. This fre-

quency increases steadily with the electronegativity of the M element within a given group of the Periodic Table. In addition, the vibrational frequency of the $[WO_4]^{2-}$ anions depends on the atomic mass of M^{z+} , which can be understood in terms of the cation environment of the $[WO_4]^{2-}$ complexes in tungstate melts. If the melt contains several types of M^{z+} cations, the cation environment distorts the cubic symmetry characteristic of a free $[WO_4]^{2-}$ complex.

ACKNOWLEDGMENTS

This work was supported by the Russian Foundation for Basic Research, project no. 01-02-16098.

REFERENCES

1. Janz, G. and James, D.W., Raman Spectra and Ionic Interactions in Molten Nitrates, *J. Chem. Phys.*, 1961, vol. 35, no. 2, pp. 739–744.
2. Child, W.C., Begun, G.M., and Smith, D.H., Raman Spectroscopy of Oxyanions in Molten Salts, *J. Chem. Soc., Faraday Trans.*, 1981, vol. 2, pp. 2237–2247.
3. Brooker, M.H. and Breeding, M.A., Significance of Both Polarizability and Polarizing Power of Cations in Nitrate Vibrational Spectra, *J. Chem. Phys.*, 1973, vol. 58, no. 12, pp. 5319–5321.
4. Walrafen, G.E., Raman Spectra of Molten Sulfates, *J. Chem. Phys.*, 1965, vol. 43, no. 2, pp. 479–482.
5. Janz, G.J., Kozlovski, T.R., and Wait, S.C., Raman Spectrum and Vibrational Assignment for Molten Thallous Nitrates, *J. Chem. Phys.*, 1963, vol. 39, no. 7, pp. 1809–1812.
6. Voron'ko, Yu.K., Kudryavtsev, A.B., Osiko, V.V., and Sobol', A.A., High-Temperature Raman Scattering Studies of Melt Structure and Crystallization Processes, *Rost Krist.*, 1988, vol. 16, pp. 178–195.
7. Lazarev, A.N., Mirgorodskii, A.P., and Ignat'ev, I.S., *Kolebatel'nye spektry slozhnykh okislov* (Vibrational Spectra of Mixed Oxides), Moscow: Nauka, 1975, p. 210.
8. Basiev, T.T., Sobol, A.A., Zverev, P.G., *et al.*, Comparative Spontaneous Raman Spectroscopy of Crystals for Raman Lasers, *Appl. Opt.*, 1999, vol. 38, no. 3, pp. 594–598.
9. Basiev, T.T., Sobol, A.A., Zverev, P.G., *et al.*, Raman Spectroscopy of Crystals for Stimulated Raman Scattering, *Opt. Mater.*, 1999, vol. 11, no. 3, pp. 307–314.
10. Basiev, T.T., Sobol, A.A., Voronko, Yu.K., and Zverev, P.G., Spontaneous Raman Spectroscopy of Tungstates and Molybdates Crystals for Raman Lasers, *Opt. Mater.*, 2000, vol. 15, no. 8, pp. 205–216.
11. Zverev, P.G., Basiev, T.T., Sobol', A.A., *et al.*, Stimulated Raman Scattering Study of Alkali Tungstate Crystals, *Kvantovaya Elektron.* (Moscow), 2000, vol. 30, no. 1, pp. 55–59.
12. Porto, S.P.S. and Scott, J.F., Raman Spectra of $CaWO_4$, $SrWO_4$, $CaMoO_4$, and $SrMoO_4$, *Phys. Rev.*, 1967, vol. 157, no. 3, pp. 716–719.

13. Banishev, A.F., Voron'ko, Yu.K., Kudryavtsev, A.B., *et al.*, High-Temperature Raman Scattering Study of Crystalline and Molten Calcium Tungstate, *Kristallografiya*, 1982, vol. 27, no. 3, pp. 618–620.
14. Morell, D.J., Cantrell, J.S., and Chang, L.L.Y., Phase Relations and Crystal Structures of Zn and Cd Tungstates, *J. Am. Ceram. Soc.*, 1980, vol. 63, no. 56, pp. 261–264.
15. Trunov, V.K., Efremov, V.A., and Velikodnyi, Yu.A., *Kristalloghimiya i svoystva dvoynykh molibdatov i vol'framatov* (Crystal Chemistry and Properties of Binary Molybdates and Tungstates), Leningrad: Nauka, 1986, p. 186.
16. Gallucci, E., Goutaudier, C., Bourgeois, F., *et al.*, Comprehensive Study of Third-Order Nonlinear Tungstates: Relationship between Structural and Vibrational Properties in Raman Shifters, *J. Solid State Chem.*, 2002, vol. 163, pp. 506–512.
17. Bell, J.V., Heisler, J., Tannenbaum, H., and Goldenson, J., A Linear Phosphoryl Absorption Relationship, *J. Am. Chim. Soc.*, 1954, vol. 76, no. 3, pp. 5185–5189.
18. Sanderson, R.T., *Polar Covalence*, New York: Academic, 1983, p. 320.
19. Bokii, G.B., *Kristalloghimiya* (Crystal Chemistry), Moscow: Nauka, 1971, p. 400.
20. Cherkasov, A.R., Galkin, V.I., Zueva, E.M., and Cherkasov, R.A., Concept of Electronegativity: Current Status, *Usp. Khim.*, 1998, vol. 67, no. 5, pp. 423–441.
21. Voron'ko, Yu.K., Sobol', A.A., Ushakov, S.N., and Tsimbal, L.I., Raman Spectra and Phase Transformations of the $MLn(WO_4)_2$ ($M = Na, K$; $Ln = La, Gd, Y, Yb$) Tungstates, *Neorg. Mater.*, 2000, vol. 36, no. 9, pp. 1130–1136 [*Inorg. Mater.* (Engl. Transl.), vol. 36, no. 9, pp. 947–953].